JOURNAL OF MATERIALS SCIENCE 16 (1981) 2583–2589

On the thermal blunting of crack tips in polymers

E. Q. CLUTTON, J. G. WILLIAMS
Department of Mechanical Engineering, Imperial College of Science and Technology, London SW7 2BX, UK

The analysis of crack tip blunting in the impact test is reviewed and the results for polymethylmethacrylate at room temperature are presented, together with more recent data for which loading times have been measured. A successful comparison is drawn between the results of impact tests at various strain rates and those of static single edge notched tests where the crack tip region is heated. Such a correlation confirms the suspected suppression of crack tip crazing owing to thermal effects.

1. Introduction

Polymers are inherently rate dependent and this factor, coupled with their low thermal conductivity, leads to accumulation of heat wherever work rates on the material are high. This is typically the case at the tips of cracks in material undergoing fracture and can therefore effect changes in the local properties, which inevitably alter material behaviour. High temperatures at the tips of fast moving cracks have been detected in many materials [1, 2] and Marshall *et al.* [3] attribute crack instabilities in polymethylmethacrylate (PMMA) to adiabatic–isothermal transitions at the crack tip.

Very recently, a thermal blunting argument has been proposed to explain the effect of increasing strain rate in impact tests on several polymers [4]. The essence of the argument is that the high strain rates occurring during initial loading produce sufficient localized heating to facilitate softening and crack tip blunting. Initiation toughness values calculated from these tests are consequently higher and may thus give a false picture of material characteristics.

The intention of this paper is to show how similar elevations in material toughness may be obtained in specimens tested at low strain rates by locally heating the crack tip region. A successful comparison between the results presented here and those of Williams and Hodgkinson [5] is achieved, lending further weight to the argument that crack tip heating is responsible for the change in material properties in a high rate fracture test.

2. Review of the impact data on PMMA

In order to prepare the ground for the comparison of data, it is essential to understand the theory of the impact test and how it may be used to study rate effects. A brief resumé of these aspects is presented here and any data used for illustration were obtained on PMMA.

As a result of discrepancies between the values quoted for the impact strengths of many materials, a great deal of work has been done, principally by Plati and Williams [6], to equate the results of impact tests on different specimen geometries, both in the Charpy and Izod modes. Consequently, a calibration factor, ϕ, was calculated for both modes to enable the energies involved to be related by the expression

$$U = G_c BD\phi + U_k \quad (1)$$

where U is the energy required to fracture a specimen of depth D, breadth B, and where U_k is the kinetic energy of the fractured sample and G_c is the strain energy release rate of fracture. A comparison of Charpy and Izod data is given by Plati and Williams [6] and a comprehensive reassessment of the subject as a whole is given by Williams and Birch [7]. The impact behaviour of PMMA over a temperature of -100 to 20° C is documented in Plati and Williams [8].

Continuing the work on impact testing of polymers, Williams and Hodgkinson [5] noticed that in each set of data some of the specimens required substantially more energy for fracture.

0022–2461/81/092583–07$02.70/0

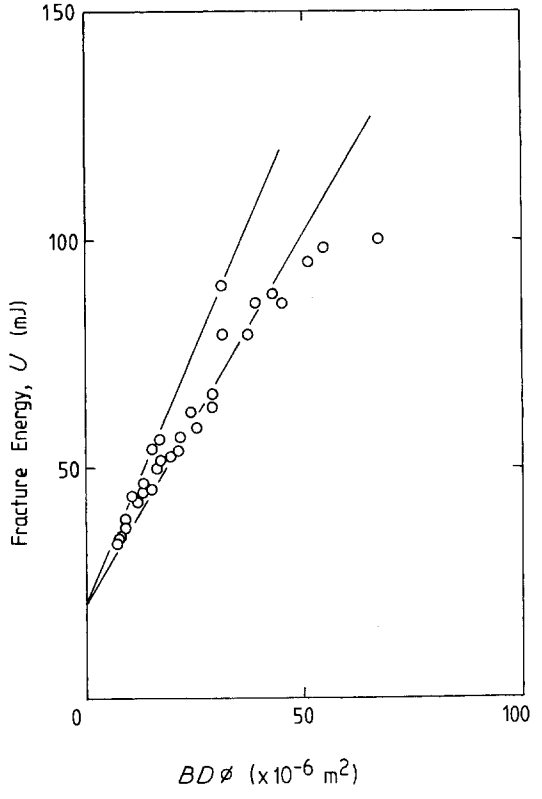

Figure 1 Impact data for PMMA at 20° C and strain rate 274 sec^{-1}.

Attributing this to strain rate dependence, they proceeded to investigate the variation of impact strength, G_c, as a function of strain rate. Fig. 1 shows typical data for PMMA at 20° C and an estimated strain rate of 274 sec^{-1}. An upper bound value is drawn in to include the higher energies.

By varying specimen dimensions and, to a lesser extent, striker impact velocity, the loading time in each impact test was varied. Short and deep specimens produce high strain rates and consequently short loading times. Fig. 2 shows the variation of toughness, G_B, with the loading time, t, calculated for each specimen. A log plot of these data revealed a dependence of the form $t^{-1/2}$.

More recent work [9] uses an improved technique enabling loads and, ultimately, fracture toughness, K_B, be to calculated. The data, when plotted on an energy basis, are indistinguishable from the earlier impact data. Previously, however, the corresponding fracture toughnesses, K_B, were calculated by assuming a modulus of 3.5 GN m^{-2}. In this recent study, the instrumentation of the test enables force–deflection behaviour to be measured and a toughness, K_B, to be determined directly. A graph of K_B against loading time (Fig. 3) was plotted showing the toughness elevation at short times.

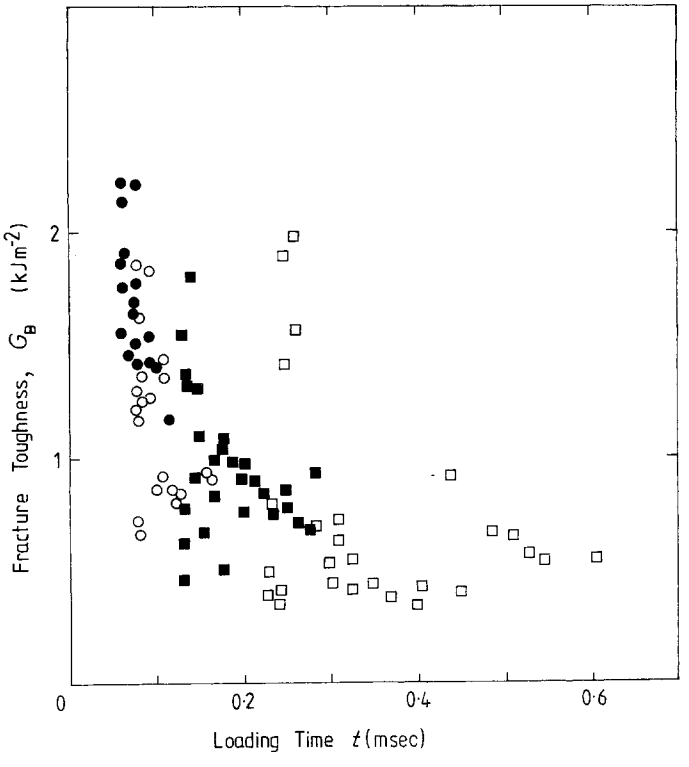

Figure 2 Variation of toughness with loading time for PMMA.

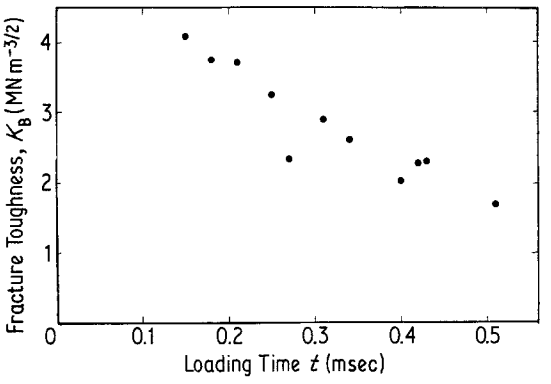

Figure 3 Variation of toughness, K_B, with loading time for the more recent data on PMMA.

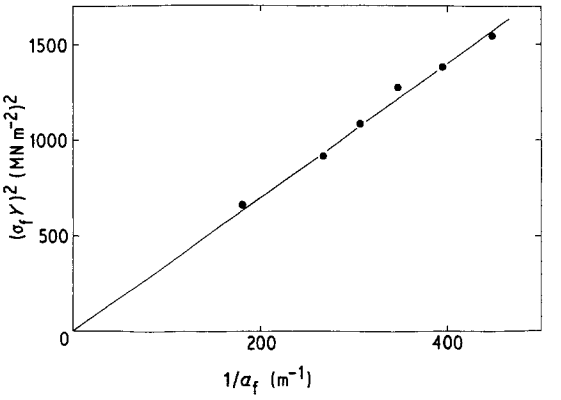

Figure 4 Typical SEN data for PMMA (40° C).

3. Experimental techniques

The standard single edge notched test-piece was used to provide the data for comparison since it provides the most expedient method for determining a stress intensity factor for the onset of unstable fracture. The capacity to test specimens at low strain rates and the ease of locally heating the crack tip were also very advantageous.

All specimens were machine notched using a sharp single point cutter which had a tip radius of approximately 25 μm as measured using a projection microscope. Extreme care was taken to ensure that crazing did not occur at the tips of the notches.

The usual techniques were employed to provide a stress intensity factor, K; that is, specimens with a range of crack lengths were tested and the failure stresses, σ_f, the final crack lengths, a_f, and the finite plate corrections, Y, were calculated. With regard to the relation

$$K = \sigma_f Y a_f^{1/2} \quad (2)$$

the stress intensity factor was determined by taking the square root of the gradient of a straight line plot of $\sigma_f^2 Y^2$ against a_f^{-1}.

3.1. Variation of toughness with temperature

In order to illustrate the effects of the blunting due to localized heating, tests were performed at various temperatures between 20 and 85° C when the whole specimen was heated. The temperature cabinet controlled the specimen temperature to within ± 0.5° C and the tests took place after an acclimatization period of 10 min. A typical graph of $\sigma_f^2 Y^2$ against a_f^{-1} is shown in Fig. 4 for PMMA at 40° C. The fracture surfaces of these specimens are typified by a "rising sun" initiation mark and there was no significant variation in the appearance of the fracture surfaces with increased temperature.

3.2. Toughness with localized heating at the crack tip

Localized heating in the specimen was effected in the following manner. A drilled hole, of radius 0.15 mm, was used as a guide for a piece of resistance wire passing through the specimen behind, but close to, the crack tip. The thickness of the wire was chosen so that good contact was made with the material and the electrical circuit, as shown in Fig. 5, was completed. The passage of a current, I, through the wire produced a steady-state temperature distribution after some 10 min had elapsed and all tests were performed in the steady-state situation. Appendix 1 presents an assessment of the temperature distribution using dummy specimens, thermocouples and a simple analysis.

Various values of current were chosen, ranging from 0.3 to 1.2 A and at each value a batch of specimens of differing notch lengths was tested. As with the isothermal tests, the load–deflection trace as recorded on the Instron machine was practically linear and a toughness corresponding to each value of current was calculated. Using the analysis of Appendix 1, the temperature at the wire was calculated for each value of current and thus each specimen is characterized by the wire temperature.

4. Analysis and results

4.1. Review of thermal blunting analysis

This analysis marries the concepts of thermal

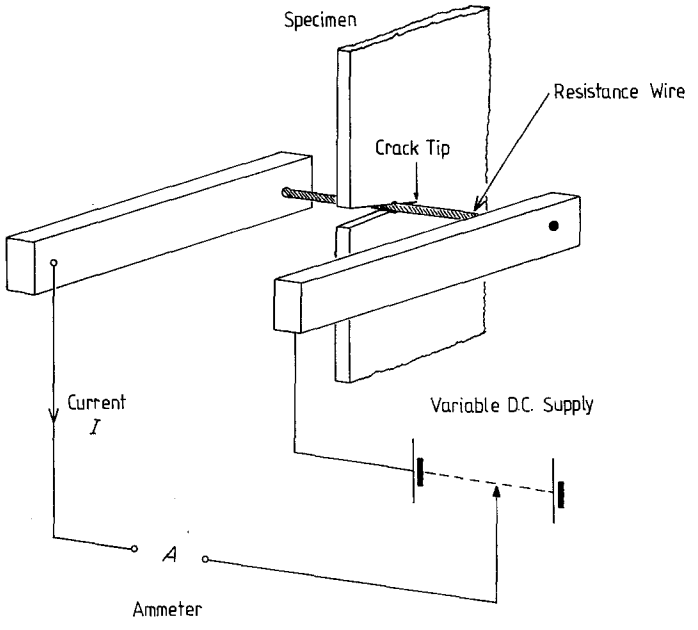

Figure 5 Diagram of electrical circuit, resistance wire and specimen.

dependence of material modulus at the crack tip with that of fracture from a notch blunted by the resulting deformation.

There is no exact solution indicating the stress field in the neighbourhood of a blunted crack and so Williams and Hodgkinson [5] examine the elastic stress ahead of an elliptical flaw. The fracture toughness, K_B, of a body containing such a flaw is directly related to the sharp notch fracture toughness, K_c. Employing a "critical stress at a critical distance" fracture criterion, their analysis leads to the following relations

$$\frac{K_B}{K_c} = 1$$

for

$$\frac{1}{(2e_y)^{1/2}}\left[\frac{p_c}{E(T)}\right] < 1$$

and

$$\frac{K_B}{K_c} = \frac{1}{(2e_y)^{1/2}}\left[\frac{p_c}{E(T)}\right] \quad (3)$$

for

$$\frac{1}{(2e_y)^{1/2}}\left[\frac{p_c}{E(T)}\right] \geqslant 1$$

where e_y is the material yield strain, p_c is the critical stress at fracture, and $E(T)$ is the modulus of the material at the crack tip.

The modulus dependence with temperature is represented by

$$E(T) = E_0\left(1 - \frac{\Delta T}{\Delta T_0}\right) \quad (4)$$

where E_0 is the modulus at temperature T_0, $\Delta T = T - T_0$ and $\Delta T_0 = T_s - T_0$, T_s being the temperature for which the modulus tends to zero. Equation 3 may now be written in the form

$$\frac{K_B}{K_c} = 1 \quad \text{for} \quad 1 - \frac{\Delta T}{\Delta T_0} > N$$

$$\frac{K_B}{K_c} = \frac{N}{1 - (\Delta T/\Delta T_0)} \quad \text{for} \quad 1 - \frac{\Delta T}{\Delta T_0} \leqslant N \quad (5)$$

where N is defined by Williams and Hodgkinson [5] as

$$N = (e_y/2)^{1/2}\frac{p_c}{p_0} = \frac{1}{(2e_y)^{1/2}}\frac{p_c}{E_0} \quad (6)$$

where p_0 is the yield stress at temperature T_0.

A simple thermal analysis relates the crack tip temperature rise, ΔT, to the loading time, t. If the energy is dissipated at a fixed rate into the zone at the crack tip, then the temperature rise is found to be proportional to $t^{-1/2}$ and the relation between the two may be written as

$$\frac{\Delta T}{\Delta T_0} = \left(\frac{t_1}{t}\right)^{1/2} \quad (7)$$

where t_1 is the minimum loading time required to reach the softening temperature, T_s. Equation 5 may now be expressed in terms of loading time, thus

$$\frac{K_B}{K_c} = 1 \quad \text{for} \quad 1-\left(\frac{t_1}{t}\right)^{1/2} > N$$
$$\frac{K_B}{K_c} = \frac{N}{1-(t_1/t)^{1/2}} \quad \text{for} \quad 1-\left(\frac{t_1}{t}\right)^{1/2} \leqslant N. \tag{8}$$

4.2. Results

The recent work of Hodgkinson and Williams [9] was carried out on specimens of similar span and depth and, although the loading times vary owing to changes in specimen compliance, the effect is not so well illustrated when the results are included with the previous data plotted together in Fig. 2. This is entirely due to the inclusion of spurious energy, such as that corresponding to multiple striking, and variations in the kinetic energy affecting the measured energy to fracture. Data which comprise Fig. 3 have been calculated from a force at fracture and the crack depth. Consequently, the behaviour shown in Fig. 3 is clearly defined as it contains none of the indeterminate effects mentioned above. Replotting these data according to Equation 8 gives a good straight line fit as shown in Fig. 6. The intercept on the $(K_B)^{-1}$ axis gives a value for $(NK_c)^{-1}$ of 0.94 and, using a minimum toughness value for K_c of 1.7 MN m$^{-3/2}$, this gives a value for N of 0.63. On the horizontal axis, the minimum loading time is given as 0.1 msec.

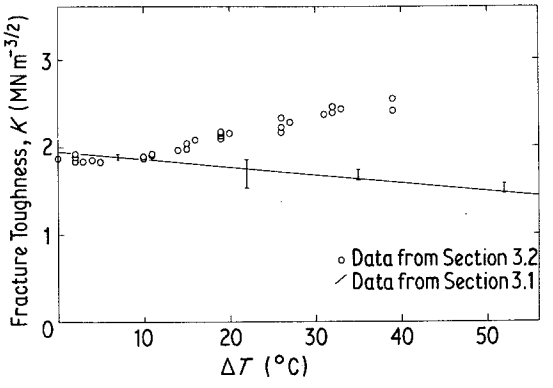

Figure 7 Comparison of data from Sections 3.1 and 3.2.

The results of Sections 3.1 and 3.2 are shown together in Fig. 7 and demonstrate the marked effect of locally heating the crack tip. Values of K_c/K_B were calculated for the data of Section 3.2 using the appropriate toughness, K_c, value from Section 3.1. K_c/K_B is then plotted against ΔT in Fig. 8 and agreement with Equation 5 is excellent with intercepts corresponding to values for N of 0.92 and for ΔT_0 of 90° C.

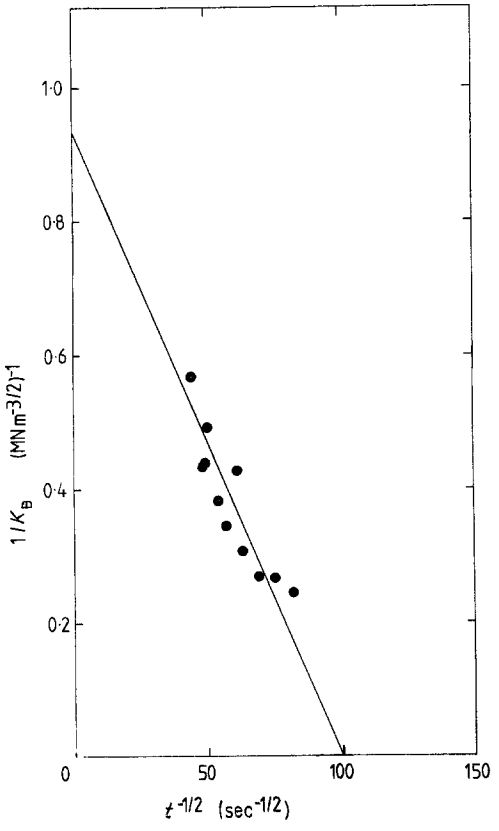

Figure 6 Graph of $(K_B)^{-1}$ against $t^{-1/2}$ for more recent impact data.

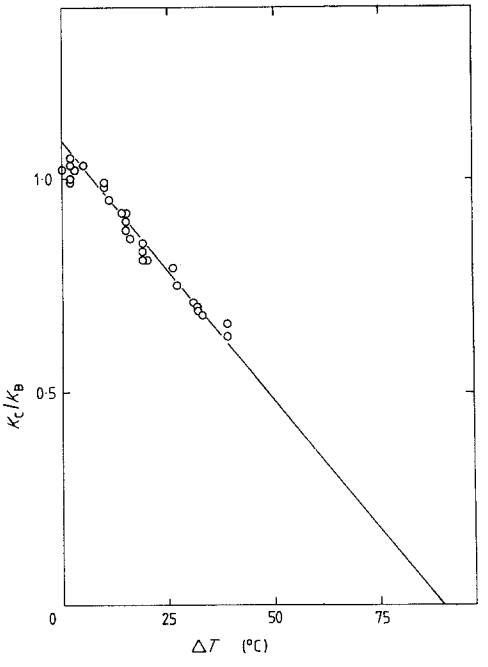

Figure 8 Graph of K_c/K_B against ΔT for the data from Section 3.

5. Discussion

There is little doubt that both the impact data [5] and the slow rate data presented here agree well with the thermal blunting analysis, the only difference being in the value of N required to fit each set of data. Recalling Equation 6, which gave N as

$$N = \left(\frac{1}{2e_y}\right)^{1/2} \frac{p_c}{E_0} \quad (6)$$

we see that e_y and p_c are assumed identical for those data presented here and the impact data. This is strictly because the heated crack tip zone is presumed responsible for a suppression of the crazing mechanism of fracture. The base modulus, E_0, however, is not the same for both sets of data owing to its rate dependence. In the work presented here, the value of E_0 appropriate to the slow rates is $5\,\mathrm{GN\,m^{-2}}$, whereas that value most applicable for the average strain rate of the impact tests is approximately $7.5\,\mathrm{GN\,m^{-2}}$. The first of these values is taken from Marshall *et al.* [3] and is a room temperature modulus suitable for instability crack speeds and the second value is an average of the calculated moduli from the recent data [9]. Assuming constancy of e_y and p_c, then the product NE_0 must remain constant. This product takes the value 4.6 for the impact data of Hodgkinson and Williams [9] and the value of 4.73 for the present work. Reconciliation of the discrepancy in N is thus effected through a rate dependent base modulus.

Three further aspects warrant attention. Firstly, the critical stresses given by Equation 6 for the quoted value of modulus are of the order of $1\,\mathrm{GN\,m^{-2}}$, whereas they were previously reported as $0.55\,\mathrm{GN\,m^{-2}}$ [5]. No insight into the stress levels at an uncrazed failure is available and both values remain unsubstantiated. Using the critical stress at a critical distance criterion, such a stress would necessitate a distance of about $1\,\mu\mathrm{m}$. Blunt notch data on polyesters and epoxies [10, 11] which do not craze are rationalized using a critical distance of approximately $1\,\mu\mathrm{m}$ which seems to suggest that the parameter of most physical relevance in the fracture criterion is that critical distance ahead of the tip.

Secondly, it was noticed during the course of this work that slow rate razor-notched specimens produced substantially lower toughness values but when tested in impact, there was no difference between machine-notched and razor-notched results [12]. This is entirely a rate effect due to the absence of slow crack growth in impact. Therefore, Fig. 7 showing the slow rate data includes the complete thermal effect.

Finally, the possible effect of a region of compressive stress at the crack tip was investigated. For both an adiabatic plug of material (a zone of material at constant elevated temperature), and a zone containing a temperature distribution such as that given in Appendix 1, an upper bound to the compressive stress is estimated to be $10\,\mathrm{MN\,m^{-2}}$. This stress will have little effect on the measured toughness, since it is local to the crack tip and negligible compared to the crack tip stress field. However, a local compressive stress such as this may be sufficient to suppress crazing.

6. Conclusions

The intention of this work was to see whether a high rate test could be simulated by artificially introducing the crack tip heating and then testing at a low rate. This has been successfully carried out and the comparison is good. The results lend a great deal of credibility to the idea that in regions of high deformation in polymers, local heating effects material properties.

A conclusion may also be drawn concerning the applicability of the "critical stress at a critical distance" criterion to the fracture of PMMA from blunt flaws. It seems very likely that when crazing is suppressed, the critical stress is in the region of $1\,\mathrm{GN\,m^{-2}}$ with a corresponding critical distance of about $1\,\mu\mathrm{m}$.

Appendix 1

Determination of crack tip temperatures due to localized heating

According to Carslaw and Jaeger [13], the temperature distribution due to cylindrical heat source (at radius, $r = 0$) in an infinite circular cylinder is given by

$$T(r) - T(r_0) = -\frac{F}{2\pi k} \ln\left(\frac{r}{r_0}\right)$$

where $T(r)$ is the temperature at radial distance r, F is the heat generation rate per unit length along $r = 0$ and k is the conductivity of the material medium. Thus, for a wire carrying a current, I, of resistance per unit length, R, radius, r_w, and surface temperature, T_w

$$T(r) = T_w - \frac{I^2 R}{2\pi k} \ln\left(\frac{r}{r_w}\right).$$

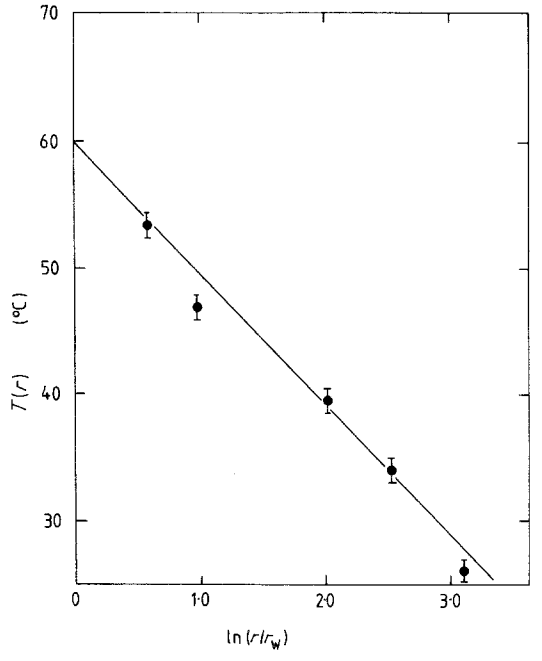

Figure A1 Temperature at distance r from crack tip against $\ln (r/r_w)$ for $I = 1.0$ A.

It was found that this relationship was very closely followed in our situation, i.e. despite a cut in the material and the presence of air, presumably owing to the low conductivity of PMMA. Fig. A1 shows temperatures recorded using thermocouples at varied distances directly in front of the crack tip. A line of gradient $I^2R/2\pi k^*$ has been fitted and the intercept $r = r_w$ gives the surface temperature of the wire. Fig. A2 shows T_w plotted against I^2 and it is found that they are proportional with, not surprisingly, an intercept at room temperature for $I = 0$.

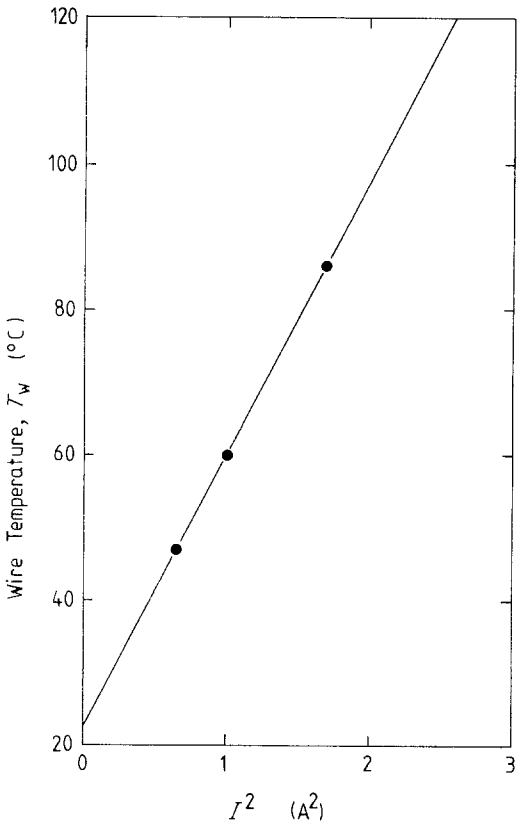

Figure A2 Surface temperature, T_w, against I^2.

References

1. K. N. G. FULLER, P. G. FOX and J. E. FIELD, *Proc. Roy. Soc. London* **A341** (1975) 537.
2. R. WEICHERT and K. SCHÖNERT, *J. Mech. Phys. Sol.* **26** (1978) 151.
3. G. P. MARSHALL, L. H. COUTTS and J. G. WILLIAMS, *J. Mater. Sci.* **9** (1974) 1409.
4. J. M. HODGKINSON and J. G. WILLIAMS, Proceedings of the Conference on Mechanical Properties of Materials at High Strain Rates, Oxford Institute of Physics Conf. Ser. No. 47 (Institute of Physics, Bristol, 1980) pp. 233–41.
5. J. G. WILLIAMS and J. M. HODGKINSON, *Proc. Roy. Soc. London* **A375** (1981) 231.
6. E. PLATI and J. G. WILLIAMS, *Polymer Eng. Sci.* **15** (1975) 470.
7. J. G. WILLIAMS and M. W. BIRCH, in "Fracture 1977", Vol. 1, Part IV, edited by D. M. R. Taplin (University of Waterloo Press, Ontario, 1977) pp. 501–28.
8. E. PLATI and J. G. WILLIAMS, *Polymer* **16** (1975) 915.
9. J. M. HODGKINSON, J. G. WILLIAMS, N. S. VLACHOS and J. H. WHITELAW, unpublished work (1980).
10. P. S. LEEVERS, unpublished work (1980).
11. A. J. KINLOCH and J. G. WILLIAMS, *J. Mater. Sci.* **15** (1980) 987.
12. J. M. HODGKINSON, unpublished work (1979).
13. H. S. CARSLAW and J. C. JAEGER, "Conduction of Heat in Solids", 2nd edn (Clarendon Press, Oxford, 1959).

Received 17 November 1980 and accepted 19 March 1981.

*The values of R and k used to calculate $I^2R/2\pi k$ were: $R = 13\ \Omega\ m^{-1}$ and $k = 0.2\ W\ m^{-1}\ K^{-1}$.